Journal of Cell Science 110, 2109-2116 (1997)
Printed in Great Britain © The Company of Biologists Limited 1997
JCS9650

Time scale dependent viscoelastic and contractile regimes in fibroblasts probed by microplate manipulation

Olivier Thoumine* and Albrecht Ott

Laboratoire de Physicochimie Curie, UMR 168 du CNRS, Section de recherche, Institut Curie, 11 Rue Pierre & Marie Curie, 75231 Paris Cedex 05, France

*Author for correspondence at present address: Laboratoire de Génie Médical, PSE-Ecublens, Ecole polytechnique Fédérale de Lausanne, CH-1015, Lausanne, Switzerland (e-mail: thoumine@ipa.dp.epfl.ch)

SUMMARY

Many essential phenomena in biology involve changes in cell shape. Cell deformation occurs in response to physical forces either coming from the external environment or intracellularly generated. In most tests of cell rheology, an external constraint is usually superimposed on an already mechanically active cell, thus the measurements may reflect both active motion and passive viscoelastic deformation. To show that active and passive processes could be distinguished on a time scale basis, we designed a novel piezo-controlled micromanipulation system to impose dynamic mechanical deformations on individual cells. Chick fibroblasts were seized between two glass microplates; one of the plates, more flexible, served as a sensor of the applied force. Controlled amounts of unidirectional compression and traction in the range of 10^{-8}-10^{-7} N were applied, using either step functions or sinusoidal signals at chosen frequencies. These tests allowed identification of three time scale dependent regimes. (1) A dominant elastic response, characterized by a linear stress-strain relationship, was especially apparent at short times (seconds); (2) A viscous behavior, characterized by force relaxation and irreversible cell deformation, was noticeable at intermediate times (minutes). Data from traction and oscillatory excitation tests were well fitted by a three-element Kelvin viscoelastic model, allowing the calculation of two elastic moduli in the range of 600-1,000 N/m^2 and an apparent viscosity of about 10^4 Pa.s. (3) A contractile regime, in which actin-dependent traction forces were developed in response to uniaxial load was apparent at longer times (several tens of minutes). These forces were in the order of 4×10^{-8} N above viscous relaxation. Thus we could distinguish, on a time scale basis, the specific contributions of passive viscoelasticity and active traction, and evaluate their mechanical characteristics within one experiment on a single cell.

Key words: Micromanipulation, Uniaxial stretch, Cell deformation, Actin, Harmonic excitation

INTRODUCTION

All cells in a mammalian organism have the ability to change shape in response to either chemical or mechanical signals. In both cases, cell deformation is a mechanical process influenced by various forces acting on the cell structure (Elson, 1988; Lauffenburger and Horwitz, 1996). These forces come from two sources: (i) mechanical fields generated by the external environment, and (ii) intracellular conversion of chemical energy into mechanical energy. Such stresses can affect fundamental cellular functions, such as migration, proliferation, and differentiation (Watson, 1991; Ingber, 1993), and may play critical roles in embryogenesis or pathology. Thus there is a need to better understand how mechanical signals collectively affect cell behavior.

Study of cell mechanics has involved the measurement of cellular deformability in response to controlled mechanical stimulations, using a variety of experimental systems. For this, two types of approaches have been followed: (i) application of global uniform loads to adherent cell populations, e.g. by fluid shear (Truskey and Pirone, 1990; Thoumine et al., 1995), basal stretch (Ives et al., 1986; Shirinsky et al., 1989), or centrifugation (Lotz et al., 1989; Thoumine et al., 1996); and (ii) local perturbation of cellular substructures (e.g. surface, pseudopods, cytoplasm), using techniques such as aspiration into micropipets (Evans et al., 1980; Evans and Yeung, 1989; Tran-Son-Tay et al., 1991; Zhelev and Hochmuth, 1994), probing surface resistance with a cell poker apparatus (Petersen et al., 1982) or an atomic force microscope (Hoh and Schoenenburger, 1994), manipulation with microneedles (Kolega, 1986; Albrecht-Buehler, 1987; Dennerll et al., 1989; Felder and Elson, 1990), and displacement of internalized (Valberg and Albertini, 1985) or surface-attached (Kucik et al., 1991; Wang et al., 1993; Choquet et al., 1997) microspheres. Taken together, those experiments have highlighted two main aspects of what are generally called passive cell mechanical properties: (i) a permanent cortical tension is present at the cell surface, which depends on the underlying actin network; and (ii) the cell interior has viscoelastic properties (Bereiter-Hahn, 1987; Dong et al., 1991) and is under positive hydrostatic pressure (Yanai et al., 1996).

In the absence of any superimposed physical stimulation,

cells already exhibit significant mechanical activity. For example, spreading of cells on culture substrates involves energy-dependent cytoskeletal motions (Bereiter-Hahn et al., 1990), stabilized by adhesive interactions. As other examples, axon extension requires microtubule polymerization (Zheng et al., 1993), whereas pseudopod formation in amoeboid cells and fibroblasts involves actin assembly (Condeelis, 1992; Mitchison and Cramer, 1996). Furthermore, cells generate traction forces during spreading and motility, possibly linked to ATP-dependent actin/myosin interactions (Harris et al., 1980; Kreis and Birchmeier, 1980; Wysolmerski and Lagunoff, 1990; Kolodney and Elson, 1995; Thoumine and Ott, 1996), and which are expressed at integral transmembrane contacts between the cell structure and the extracellular environment (Schiro et al., 1991; Wang et al., 1993). Some authors have estimated the forces linked to these active processes, for example during leucocyte phagocytosis (Evans et al., 1993), fibroblast spreading (Harris et al., 1980), or keratocyte locomotion (Lee et al., 1994).

Both active (polymerization, traction) and passive (adhesion, elastic and viscous deformations) processes are likely to contribute to cell shape changes observed experimentally, thereby influencing the mechanical measurements. For example, the strength of the cell cortex is linked to the degree of spreading (Wang and Ingber, 1994), being thereby under the control of adhesion. Therefore, it is difficult to deduce from these mechanical tests which part of the cellular response is due to passive deformation in response to the applied load, and which part is caused by active motion. One way to identify the specific mechanical contribution of each of these phenomena is to carefully analyze the time scale of those events, with a mechanical test allowing precise adjustment of the loading rate. We designed a novel micromanipulation system to impose uniaxial deformation to individual cells at varying frequencies, allowing global measurements of cell structural properties. We identified three distinct time scale dependent mechanical regimes in fibroblasts: elastic, viscous, and contractile. We interpret the measurements using a mechanical model and discuss the different regimes in relation to the various constituents of the cellular structure.

MATERIALS AND METHODS

Cell culture

Fibroblasts were isolated from the hearts of 10-day-old chick embryos as described (Thoumine and Ott, 1996). Cells were cultured in minimal essential medium (MEM) supplemented with 50 i.u./ml penicillin, 0.05 mg/ml streptomycin, 2 mM L-glutamine, and 10% fetal bovine serum (FBS). Cells were used at passages 3 to 6. Cell culture reagents were purchased from Biological Industries (Israel).

Microinstrument preparation

Microplates of varying stiffnesses were fabricated from $0.075 \times 1 \times 100$ mm borosilicate ribbon pieces (VitroCom, Mountain Lakes, NJ, USA) using a micropipet puller (Sutter Instrument Co., Novato, CA, USA). To make them adhesive, microplates were treated with sulfochromic acid for 2 hours at 60°C, rinsed with water, incubated in 2% 3-aminopropyltriethoxysilane, 90% ethanol, 8% water for 2 hours at room temperature, finally rinsed in ethanol, let dry, and stored in sealed tubes for up to 4 days. Before manipulation, instruments were dipped in 2% glutaraldehyde, 98% water for 1 hour at room temperature and rinsed with water. To make them non-adhesive, microplates were incubated in MEM containing 10% FBS for 1 hour at room temperature. Chemical reagents were purchased from Sigma (St Louis, MO, USA).

Experimental set-up

Microplates, one rigid, the other flexible, were held by home-made steel arms connected to two micromanipulators (Physik Instrumente, Waldbronn, Germany). These were mounted on each side of the stage of an inverted microscope (Zeiss, Oberkochen, Germany) placed on an anti-vibration table (Newport, Irvine, CA, USA). Fine displacement of the rigid microplate in the *y*-axis (Fig. 1) was achieved using a closed-loop piezoelectric translator (Physik Instrumente) controlled by a computer through a digital-analog interface (LabView software, National Instruments, Austin, TX, USA), with input signals which could be freely chosen.

Micromanipulation

Cells were detached from tissue culture plastic wells by a 1 minute treatment with 0.05% trypsin, 2.3 mM EDTA in PBS, resuspended in MEM containing antibiotics, L-glutamine and 20 mM Hepes, then placed in a manipulation chamber. A rigid and adhesive microplate was positioned beneath a fibroblast settling down by gravity. Stable adhesion occurred within a few seconds after contact between the cell and the microplate. The microplate was turned by a 90° angle to visualize the cell from the side, and the cell was placed against either a non-adhesive (for compression) or adhesive (for traction and sinusoidal perturbation) flexible microplate. FBS (1%) was then added to the suspension. Either step or sinusoidal input signals to the piezoelectric element were used to perform compression, traction, or oscillatory deformation around the initial shape of the cell. Tests lasted from 35 to 75 minutes; they were done at room temperature.

Force calibration

Reference microneedles pulled from 1 mm diameter glass rods (Clark Electromedical Instruments, Pangbourne, UK) were positioned at a low angle onto the stage of a 0.01 mg precision analytic balance (Ohaus, Florham Park, NJ, USA), using a micrometer-driven translation stage (Newport). They were lowered by vertical steps of 10 μm. The relationship between the weight given by the balance and the height read on the micrometer was very linear (up to 100 μm), and the corresponding slope was taken as the sensitivity of the micro-

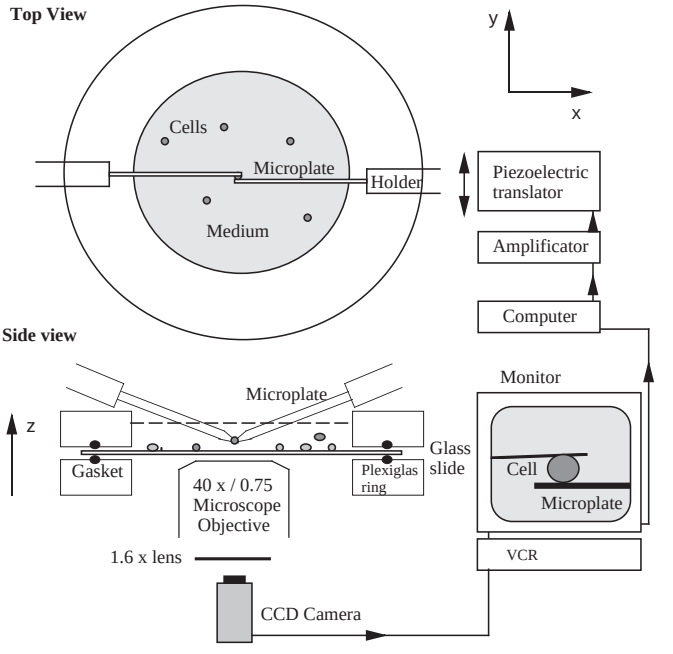

Fig. 1. Schematic diagram of the experimental set-up.

needle. At the end of each experiment, such a reference microneedle (sensitivity 5.6+0.5 10^{-8} N/μm) was placed onto the tip of the flexible microplate, and moved by 2.5 μm increments with the piezoelectric translator (up to 20 μm). The relationship between the deflections of the two instruments was linear, allowing determination of microplate sensitivity (10^{-9}-10^{-8} N/μm).

Data acquisition

Sequences of cell deformation under brightfield illumination magnified with a ×40/0.75 objective and a ×1.6 Optovar lens were filmed with a CCD camera (Cohu Inc., San Diego, CA, USA) connected to a video cassette recorder (Panasonic, Matsuhita Electric Industrial Co., Osaka, Japan). Images were digitized using a Power MacIntosh computer equipped with a frame grabber card (Scion Co., Frederick, MD, USA), and analyzed using NIH Image software. The following parameters were measured over time (t): (i) cell dimensions in the directions parallel ($d_{\parallel}$) and perpendicular ($d_{\perp}$) to the plane of the microplates, which served to calculate a shape index ($d_{\perp}/ d_{\parallel}$) that quantitatively characterizes cell flattening or elongation; and (ii) deflection of the flexible microplate. Errors, taking into account optical resolution and low frequency vibrations, were in the order of 0.4 μm. The force applied on cells was calculated by multiplying the flexible microplate deflection by its sensitivity obtained from the calibration procedure. Deflection of the rigid microplate, around 100 times stiffer than the flexible instrument, was neglected. The error in force measurements, including detection of the microplate position, thermal drift of the instruments, and calibration procedure was about 10%. Uniaxial stress was taken as $\sigma(t) = 4 f(t)/\pi d_{\parallel}^2$ (ratio of the force f to the cross-sectional area of the cell), and strain was taken as $\varepsilon(t) = d_{\perp}(t)/d_{\perp}(0)-1$.

RESULTS

A suspended fibroblast was seized with a rigid glass microplate chemically treated so that amine groups on cell surface proteins covalently bound the glass surface. The free extremity of the cell was then placed against another microplate, more flexible, which served as a force sensor. Experiments of compression, traction, or oscillatory perturbation were then performed as described below.

Compression

When compressed between two microplates, fibroblasts flattened within seconds (Fig. 2A,B), as characterized by a large and rapid decrease in shape index (ratio of cell length to width) (Fig. 2D). Concomitantly, the uniaxial force transmitted by the cell body rapidly increased up to about 8×10^{-8} N (Fig. 2E). As load was maintained, a partial (about 20%) and progressive force relaxation was observed over a 30 minute observation period, coincident with cells becoming slightly more flattened (Fig. 2D,E). When the rigid microplate was pulled back, the force instantly dropped to zero (Fig. 2E) and cells regained their original round morphology within 30 seconds (Fig. 2C,D). A small remaining cell deformation (Fig. 2C) was sometimes present after removal of the load, corresponding to a shape index slightly lower than at time 0 (Fig. 2D); this was probably due to cell spreading on the rigid microplate. To evaluate cell spreading dynamics on microplates, control experiments were performed in which fibroblast populations were plated on glass coverslips treated identically to the microinstruments (silane + glutaraldehyde): it took cells an average of 4 hours to completely spread on these coverslips (not shown), thus spreading should not severely interfere with the measurements when the duration of the mechanical tests is kept below the hour.

Traction

Two adhesive microplates were used to seize a fibroblast from both sides (Fig. 3A,B). After an incubation time sufficient to reach a stable and symmetric adhesion (Fig. 3B), microplates were pulled apart in a few seconds. This produced a major cell elongation (Fig. 3C), characterized by a jump in shape index (Fig. 3E) and accompanied by a rapid increase in tension up to 11×10^{-8} N (Fig. 3F). Then, the uniaxial force transmitted by the cells decreased steeply during the first few minutes after initial stretch to a minimal value of about 7×10^{-8} N (Fig. 3F): this corresponded to a further increase in cell elongation (Fig. 3E). As stretch was maintained, the force did not continue to decrease in a monotonic fashion: instead, starting between 5 and 15 minutes after the initial stretch (depending on the cell), the force was observed to increase progressively up to a plateau around 9×10^{-8} N, which was reached in about 40 minutes (Fig. 3F). Force generation was associated with a contraction of cell bodies (Fig. 3D) and a decrease in shape index (Fig. 3E). In the presence of 0.2

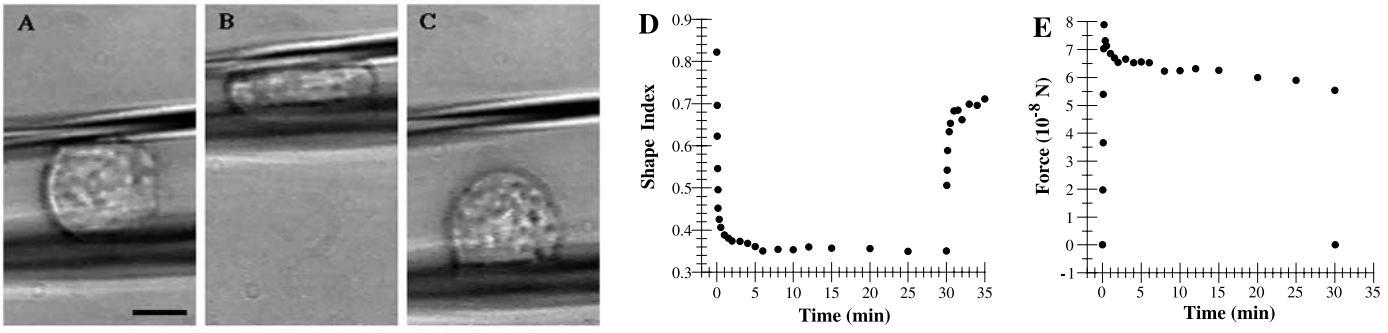

Fig. 2. Compression experiment. A rounded fibroblast (center) seized with an adhesive rigid microplate (bottom contour) was placed into contact with a non-adhesive, flexible microplate (top contour), whose deflection was used to determine the force applied. At time 0, the rigid microplate was displaced 12 μm in 10 seconds in the y direction (upward), maintained at this position for 30 minutes, then quickly moved downward to its original position. Cell relaxation was filmed for another 5 minutes. A typical cell is shown at times 0 minutes (A), 15 minutes (B), and 35 minutes (C). Bar, 5 μm. (D) Shape index versus time. (E) Uniaxial force applied, versus time. Traces represent averages of 15 cells. Standard deviations represent, in proportion of mean values, 10-39% (shape index) and 26-45% (force).

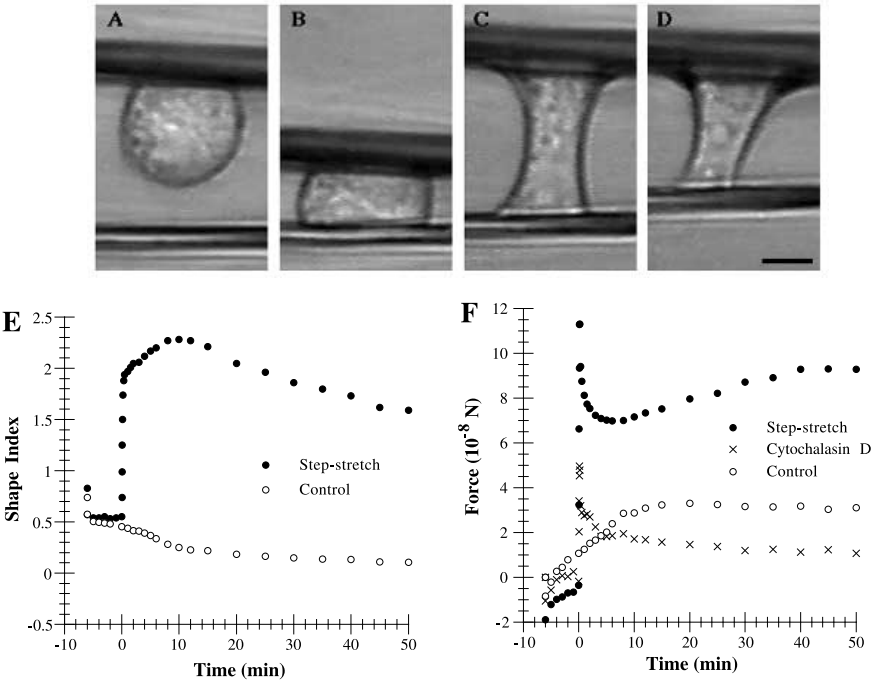

Fig. 3. Traction experiment. A fibroblast adherent to an adhesive and rigid microplate (top), was lowered 3 μm onto an adhesive, flexible microplate (bottom), and incubated for 6 minutes. At time 0, the rigid microplate was moved upward through 12 μm in 10 seconds, maintained at this position for 1 hour, then moved further away until rupture of adhesion (not shown). A typical cell is shown at times −6 minutes (A), 0 minutes (B), 10 minutes (C) and 45 minutes (D). Bar, 5 μm. (E) Shape index versus time. (F) Uniaxial force developed, versus time. In control experiments, the cell was just laid onto the flexible microplate, and no stretch was applied. In some experiments, 0.2 μg/ml cytochalasin D was added to the medium at the start of the manipulation. Traces represent averages of, respectively, 12 (Step-stretch), 4 (Control), and 6 (Cytochalasin D) cells. Standard deviations are 13-58% for shape index and 48-73% for uniaxial force.

μg/ml cytochalasin D, the force developed was significantly lower than in the untreated condition and progressively relaxed to zero (Fig. 3F). Under no external force (control condition), cells slowly spread between the two adhesive glass substrates, as demonstrated by a progressive decrease in shape index (Fig. 3E), thus pulling on the flexible microplate and developing tension which reached a plateau around 3.5×10^{-8} N (Fig. 3F).

The force relaxation and cell elongation in response to stretch before the active cellular contraction was modeled using a minimum number of viscoelastic elements (Fung, 1981; Dennerll et al., 1989; Tran-Son-Tay et al., 1991). The most appropriate was a Kelvin model, a first spring in parallel with a serial combination of a second spring and a dashpot (Fig. 4A). The deformation occurring during initial application of stress ($0 \le t \le 8$ seconds, where t is the time) was too rapid to exhibit viscous behavior, therefore the relationship between stress (σ) and strain (ε) was linear (Fig. 4B):

$$\sigma\,(t) = (k_0 + k_1)\,\varepsilon\,(t), \qquad (1)$$

where k_0 and k_1 represent the stiffnesses of the first and second springs, respectively (both springs contribute to elongation). The later phases of cell deformation (10 seconds $\le t \le t_c$, where t_c is the time at which contraction begins and slightly varies from cell to cell) were described by the following time-dependent equation between stress and strain for this particular model (Fung, 1981):

$$\sigma + \mu/k_1\,\sigma' = k_0\,\varepsilon + \mu\,(1 + k_0/k_1)\,\varepsilon', \qquad (2)$$

where the primes designate time derivatives and μ is the viscosity of the dashpot. Since in this time interval cell elongation was less marked than force diminution (see Fig. 3D), we approximated that force relaxation occurred at constant strain, i.e. $\varepsilon' = 0$. We thence obtained the following solution of equation (2):

$$\sigma\,(t) = \varepsilon_0\,(k_0 + k_1\,e^{-t/\tau}), \qquad (3)$$

where the relaxation time τ equals μ/k_1, and ε_0 is the strain right after initial stretch (t = 10 seconds). Fitting the data points for each individual cell with these mathematical expressions allowed estimation of the model parameters (Fig. 4B,C). We found $k_0 = 9.6 \pm 3.9\ 10^2$ N/m^2 and $k_1 = 5.1 \pm 3.8\ 10^2$ N/m^2 for the spring elastic moduli (95% confidence intervals calculated from a Student distribution, $n = 11$), and an average viscosity $\mu = 1.3\times10^4$ Pa.s (values scattered between 10^3 and 10^5 Pa.s), corresponding to relaxation times τ around 40 seconds.

Oscillatory perturbation

Fibroblasts were seized between a rigid and a flexible adhesive microplates and exposed to alternative traction and compression, using a sinusoidal waveform of amplitude ± 12 μm at four different frequencies (corresponding to a period T of 4, 40, 400 or 4,000 seconds). Only uniaxial forces were derived from these experiments. The force response curve over time closely followed the excitation signal: it was well fitted by two independent half sinusoids, one for the traction part, the other for the compression part, with slightly different amplitudes and phases (Fig. 5A). The long term response (T = 4,000 seconds) deviated slightly from a pure sinusoid (Fig. 5A), indicating nonlinearity. Indeed, cell contraction events are somewhat erratic, and the resulting force is not necessarily proportional to the excitation signal. The peak amplitude in traction (t/T = 0.25) first decreased with the stimulation period (from T = 4 to 400 seconds), then increased again at longer periods (T = 4,000 seconds). This corresponded precisely to the phenomena observed in step-stretch experiments (Fig. 3F), namely force relaxation during the first few minutes followed by force generation on a time scale of one hour. The phase difference between the excitation and response signals was found to follow a bell-shaped curve, both for traction and compression

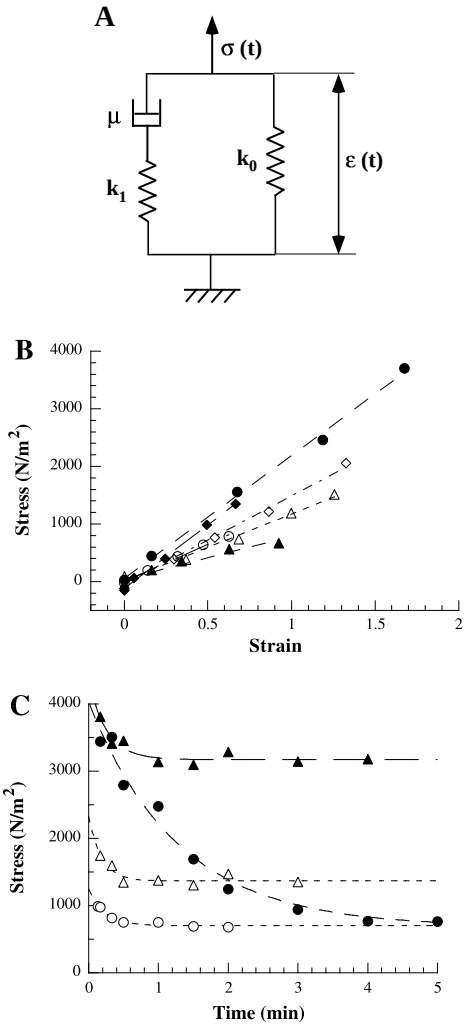

Fig. 4. Viscoelastic model and parameters adjustment. (A) Kelvin body, also called standard linear solid model. (B) Stress-strain plot of the initial elastic part of the deformation ($0 \leq t \leq 8$ seconds), for six individual cells. The slope given by linear fits (dashed lines) equals the sum $k_0 + k_1$. (C) Stress relaxation versus time for four individual cells. Exponential fits (dashed lines) through the data points ($0 \leq t \leq t_c$) give the time constant τ and the equilibrium value k_0.

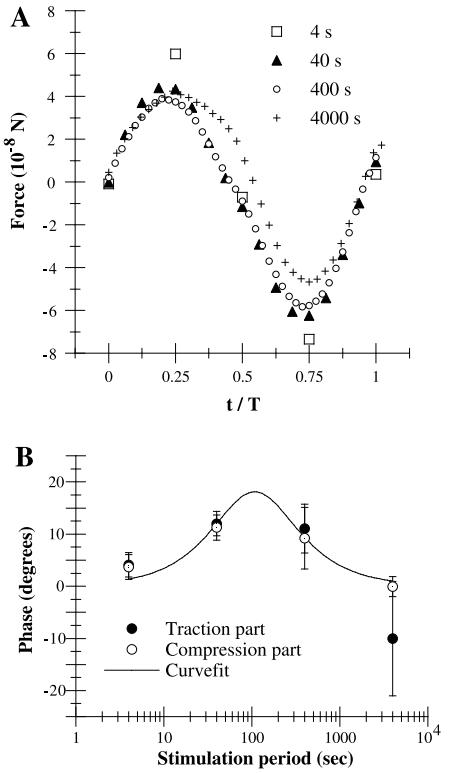

Fig. 5. Sinusoidal perturbation. (A) Uniaxial force versus dimensionless time t/T, where T is the stimulation period (see legend panel). Traces represent averages of 6-11 cells. Standard errors represent 30-50% of the mean values. For each cell and frequency, compression and traction parts were independently fitted by $f(t) = a + b \sin(2\pi t/T + \phi)$, where f is the force, and a, b, and ϕ are adjustment parameters. (B) The phase (ϕ) for both compression and traction parts is plotted versus the stimulation period. Bars indicate 95% confidence intervals calculated from a Student distribution. Although only its mean value is presented, ϕ actually varies with time: at half period, it reaches a maximum for T = 40 seconds and 400 seconds and a minimum for T = 4,000 seconds, corresponding to a maximal lag between the viscous and active response curves at t = T/2 in (A). The absolute value of the phase is generally lower in the compression part: for intermediate frequencies, this is due to weaker viscous effects (see Figs 2 and 3); at low frequency (T = 4,000 seconds) the already contracted cells behave as rigid bodies, thus transmitting the force synchronously. The plain line represents a mathematical expression of the form $\varphi = \text{Arctan}[c\omega/(1 + d\omega^2)]$, fitted through all experimental points. The adjustment constants are: $c = \mu/k_0 = 11$ seconds, and $d = \mu^2/k_0k_1(1 + k_0/k_1) = 295$ seconds^2 (see Equation 6). Note that the phase at longer periods (T = 4,000 seconds) in the traction part was lower than that predicted by the viscoelastic model.

periods (Fig. 5B): it was at a value close to 0° for T = 4 seconds, then reached positive values at intermediate frequencies (T = 40 and 400 seconds), i.e. the force response was in advance of the excitation signal thus shifted to the left (Fig. 5A). The phase finally became negative at longer periods (Fig. 5B, T = 4,000 seconds), i.e. the force response came later, thus the curve was shifted to the right of the excitation signal (Fig. 5A).

The same viscoelastic model described in the preceding paragraph was used to predict cell behavior in response to sinusoidal perturbation. Stress and strain were written in complex forms:

$$\varepsilon(t) = \varepsilon_1 e^{i\omega t}, \quad (4)$$

and

$$\sigma(t) = \sigma_1 e^{i(\omega t + \varphi)}, \quad (5)$$

where ω is the pulsation of the oscillations ($\omega = 2\pi / T$), ε_1 and σ_1 designate strain and stress amplitudes, respectively (they depend on ω), and φ is the phase difference between the excitation signal and the stress response curve (the phase of the strain was taken as zero, again assuming that cell deformation follows the imposed microplate displacement). Replacing into equation (2) and symplifying, we obtained an expression for $e^{i\varphi}$, from which we deduced:

$$\varphi = \text{Arctan}[\mu\omega / (k_0 + (\mu^2/k_1)(1 + k_0/k_1)\omega^2)]. \quad (6)$$

When plotted versus the stimulation period this function exhibits a bell shape, which can be adjusted through the experimental data (Fig. 5B): the curvefit imposes two constraints on

the model parameters (μ, k_0, k_1), as described in the legend to Fig. 5B. Among the parameters estimated from traction tests, k_0 was the most reliable: therefore, we kept $k_0 = 9.6\times10^2$ N/m^2 and obtained two new values for k_1 ($8.4 \pm 3.4\ 10^2$ N/m^2) and μ (1.1×10^4 Pa.s), close to those obtained from traction tests.

DISCUSSION

We report here experiments aimed at discriminating between the active and passive responses of cells to mechanical perturbations, on a time scale basis. We used a new microplate manipulation technique, allowing excitation of the cell structure at varying time periods and measurements of overall cell mechanical properties at the individual level.

Advantages and limits of the experimental system

Advantages of this technique are its simple geometry and a precise simultaneous control of force and deformation. Compared to the apparatus of Hiramoto (1963) to compress sea urchin eggs, we can examine the cellular response to both compressive and tensile loads, and manipulate much smaller cells like the chick fibroblasts used here, which were chosen in order to allow eventual correlation of our mechanical measurements to already existing qualitative data on the structural, adhesive, and migratory properties of these cells (Harris, 1990). Moreover, we manipulate living cells, in contrast to older techniques used to measure adhesion between two cells, which involved piercing the cells with microneedles (Coman, 1944; Hubbe, 1981). A further advantage of the set-up is that, by making repeated experiments on the same cell, one may in the future directly address the question of whether cells retain a biochemical or rheological memory of past perturbations. One limit of our system is that the microplates used to manipulate cells are very adhesive and thereby promote cell spreading: the problem is partly overcome by the fact that spreading is progressive and occurs on a time scale slower than that required for deformation tests. Another drawback is that force and deformation are not independent: an improved version of the set-up solving this issue is currently being designed. Nevertheless, the system in its present form allowed us to make reliable measurements on the three following time-scale dependent regimes.

Elastic behavior

Elasticity was a dominant feature and especially apparent at short time scales (order of seconds). During compression, fibroblasts behaved like rubber balls: they rapidly flattened upon imposition of force, retained this shape as load was maintained, then quickly regained their original rounded morphology when the force was removed. The linear increase of stress with strain during the first seconds of traction tests also revealed elastic behavior. Consistent with these observations, the force response to sinusoidal excitation showed a phase close to zero at high frequencies, where relatively high forces were developed. In addition, the phase difference between the excitation and response signals reached a maximum of only 10-15°, showing that the cellular response is dominated by elastic effects. (For comparison, a perfectly elastic solid would show no phase shift, whereas a Newtonian fluid would exhibit a 90° phase shift). Several cellular components may contribute to these elastic features, for example the actin-rich cortex (Kolega, 1986; Evans and Yeung, 1989) which is thought to be responsible for shape recovery of neutrophils after large deformation into micropipets (Tran-Son-Tay et al., 1991; Zhelev and Hochmuth, 1994).

Viscous response

At intermediate time ranges (several minutes), viscous dissipation appeared. In traction tests, a high viscous component was apparent, since uniaxial force decreased exponentially during the first few minutes after initial stretch, allowing the use of a Kelvin viscoelastic model. Accordingly, in sinusoidal stimulation at intermediate frequencies (T = 40 and 400 seconds) the peak force was lower than at high frequency (T = 4 seconds), and the phase between the force response and the excitation signal reached its maximum. This corresponds to high internal friction and is well predicted by the Kelvin model placed under harmonic excitation (Fung, 1981). Also, when fibroblasts were pulled until detachment from the flexible microplate at the end of traction tests, it took them over a few minutes to get back to their original shapes (data not shown), indicating a plastic deformation. All these phenomena reveal a fluid character, which may be attributed to viscous properties of the cell interior, i.e. the cytoplasm (Bereiter-Hahn, 1987; Evans and Yeung, 1989; Tran-Son-Tay et al., 1991) or the entangled cytoskeleton (Janmey, 1991; Ziemann et al., 1994). In compression tests, we observed a partial force relaxation over time, coincident with cells becoming more flattened, but it obviously was a minor component of cell behavior. This difference of mechanical behavior in compression and traction may be interpreted by considering the role of the nucleus: in traction, it does not interfere with cell deformation, e.g. with cytoplasmic flow or cytoskeletal remodeling. But in compression, the cell nucleus is squeezed between the two microplates and may greatly contribute to resisting deformation. Future investigations of such phenomena using this micromanipulation system may lead to indirect but reliable measurements of the intrinsic mechanical properties of the nucleus.

Contractile behavior

At longer observation times, fibroblasts showed a contractile activity. This was obvious from traction tests: about 10 minutes after initial stretch cells started to contract, developing tension up to a plateau around 4×10^{-8} N above viscous relaxation, which was reached in less than an hour. When a sinusoidal perturbation was applied to cells at such frequency (T = 4,000 seconds) the force curve exhibited a higher amplitude than at intermediate frequencies (T = 40 and 400 seconds), revealing force generation. Moreover, it showed a negative phase difference with respect to the stimulation, not predicted by the viscoelastic model: as the excitation amplitude decreased, cells continued pulling thereby increasing the force and shifting the response curve to the right. To put these findings together, cell traction may be schematized as a contractile element to be added in parallel to the three-element viscoelastic model already described. In agreement with the results, this active element may be phenomenologically characterized by an exponential relationship between traction force (F_a) and time (t): $F_a = F_0\ (1-e^{-t/\tau})$, where F_0 is a plateau force ($t \rightarrow \infty$) in the order of 5×10^{-8} N, and τ is a time constant of about 15 minutes.

The active tension generated after polarization by the inital

traction is linked to a progressive organization of the cellular structure: cells which lysed while being stretched did not develop tension thereafter, and cells treated with cytochalasin D were not able to contract, showing that intact actin filaments were necessary to force generation. Moreover, when cells were further stretched after a traction test of one hour, they had become noticeably stiffer than at the beginning of the experiment (data not shown). Such stiffening, or reinforcement, of the cell structure upon application of a load, has been reported to occur at the integrin cytoskeletal lingage in two other experimental systems (Wang et al., 1993; Choquet et al., 1997). Treatment of fibroblasts with nocodazole or taxol did not significantly affect the cellular response to the traction tests (data not shown), indicating that microtubules do not play a major mechanical role under these experimental conditions.

Validity of the mechanical measurements

The stresses applied to deform chick fibroblasts were in the range of 1.2-1.7×10^{-9} N/μm^2 for traction tests and 3-4×10^{-10} N/μm^2 in compression experiments. For comparison, stresses necessary to aspirate neutrophils (Evans and Yeung, 1989) or endothelial cells (Sato et al., 1987) into micropipets are around 10^{-10} N/μm^2. Those involved in cell poking experiments range from 1-5×10^{-9} N/μm^2 (Petersen et al., 1982; Hoh and Shoenenberger, 1994). Moreover, the forces used to induce viscoelastic deformation of fibroblast protrusions (Felder and Elson, 1990) or neurites (Dennerll et al., 1989) with microneedles are, respectively, 1.5-3×10^{-10} N and 10^{-10}-10^{-9} N: these forces correspond to stresses close to those reported here, assuming a microneedle-to-cell surface contact area of between 0.1 and 1 μm^2.

The apparent viscosity we measured here (~10^4 Pa.s) is consistent with viscosity values obtained for fibroblasts (O. Thoumine and A. Ott, unpublished work) and endothelial cells (Sato et al., 1990) from analysis of micropipet aspiration tests. This viscosity of 10^4 Pa.s is about 2 orders of magnitude larger than that reported for neutrophils (typically 100-300 Pa.s at room temperature) (Evans and Yeung, 1989; Zhelev and Hochmuth, 1994): this is likely to reflect the higher degree of structural organization of fibroblasts and endothelial cells versus leucocytes. In addition, a great variability in viscosity measurements has been noted previously (Bereiter-Hahn, 1987; Valberg and Feldman, 1987), which may depend on the use of different cell types and techniques of evaluation, as well as on shear rate and temperature dependence. The elastic parameters we measured for chick fibroblasts fall in the range of values obtained using other techniques and cell types (Erickson, 1980; Sato et al., 1990).

Finally, the tractional forces we report in this study (around 4×10^{-8} N) are quantitatively comparable to those exerted by spreading fibroblasts (Harris et al., 1980), locomoting keratocytes (Lee et al., 1994), or phagocytes engulfing pathogens (Evans et al., 1993), pointing to the existence of universal mechanisms for cell contraction, whether based on motor proteins (Kreis and Birchmeier, 1980) or on cytoskeletal network solation (Kolega et al., 1991).

In summary, we have demonstrated a time scale dependent discrimination between passive viscoelasticity and active traction in fibroblasts. These findings suggest that the time scale and the rate of the applied load are critical determinants of the output of mechanical tests performed on cells. Further studies are planned to follow, including visualization of fluorescently labeled cytoskeletal filaments during deformation and systematic perturbation of the mechanically important structural elements, which should reveal details on the relationship between molecular structure and mechanics. As literature grows on thermodynamic and mechanical properties of cellular constituents (Janmey, 1991), one may hopefully establish a link between the rheology of cells and the physics of their structural components, and build a general mathematical model of cell morphology in relation to the reality of biological processes.

This work was supported by funds from Institut Curie, CNRS, Association pour la Recherche contre le Cancer, and Fondation pour la Recherche Médicale. The authors thank P. Cluzel and J. Davidovits for the glass coating protocol, O. Cardoso and R. David for help with image analysis, F. Amblard, D. Chatenay, G. Debregeas, F. Graner, F. Heslot, J. Prost, D. Riveline, and A. Simon for stimulating discussions and F. Juelicher for critical reading of the manuscript.

REFERENCES

Albrecht-Buehler, G. (1987). Role of cortical tension in fibroblast shape and movement. *Cell Motil. Cytoskel.* **7**, 54-67.

Bereiter-Hahn, J. (1987). Mechanical principles of architecture of eucaryotic cells. In *Cytomechanics: the Mechanical Basis of Cell Form and Structure* (ed. J. Bereiter-Hahn, O. R. Anderson and W.-E. Reif), pp. 3-30. Berlin: Springer-Verlag.

Bereiter-Hahn, J., Lück, M., Miebach, T., Stelzer, H. K. and Vöth, M. (1990). Spreading of trypsinized cells: cytoskeletal dynamics and energy requirements. *J. Cell Sci.* **96**, 171-188.

Choquet, D., Felsenfeld, D. P. and Sheetz, M. P. (1997). Extracellular matrix rigidity causes strengthening of integrin-cytoskeletal linkages. *Cell* **88**, 39-48.

Coman, D. R. (1944). Decreased mutual adhesiveness, a property of cells from squamous carcinomas.*Cancer Res.* **4**, 625.

Condeelis, J. (1992). Are all pseudopods created equal? *Cell Motil. Cytoskel.* **22**, 1-6.

Dennerll, T., Lamoureux, P., Buxbaum, R. E. and Heidemann, S. R. (1989). The cytomechanics of axonal elongation and retraction. *J. Cell Biol.* **109**, 3073-3083.

Dong, C., Skalak, R. and Sung, K.-L. P. (1991). Cytoplasmic rheology of human neutrophils. *Biorheology* **28**, 557-567.

Elson, E. L. (1988). Cellular mechanics as an indicator of cytoskeletal structure and function. *Annu. Rev. Biophys. Biophys. Chem.* **17**, 397-430.

Erickson, C. A. (1980). The deformability of BHK cells and polyoma virus-transformed BHK cells in relation to locomotory behavior. *J. Cell Sci.* **44**, 187-200.

Evans, E. A., Kwok, R. and McCown, T. (1980). Calibration of beam deflection produced by cellular forces in the 10^{-9}-10^{-6} gram range. *Cell Biophys.* **2**, 99-112.

Evans, E. A. and Yeung, A. (1989). Apparent viscosity and cortical tension of blood granulocytes determined by micropipet aspiration. *Biophys. J.* **56**, 151-160.

Evans, E., Leung, A. and Zhelev, D. (1993). Synchrony of cell spreading and contraction forces as phagocytes engulf large pathogens. *J. Cell Biol.* **122**, 1295-1300.

Felder, S. and Elson, E. L. (1990). Mechanics of fibroblast locomotion: quantitative analysis of forces and motions at the leading lamellas of fibroblasts. *J. Cell Biol.* **111**, 2513-2526.

Fung, Y. C. (1981). *Biomechanics: Mechanical Properties of Living Tissues*. Berlin: Springer-Verlag.

Harris, A. K., Wild, P. and Stopak, D. (1980). Silicone rubber substrata: a new wrinkle in the study of cell locomotion. *Science* **208**, 177-179.

Harris, A. K. (1990). Protrusive activity of the cell surface and the movements of tissue cells. In *Biomechanics of Active Movement and Deformation of Cells*. NATO ASI series (ed. N. Akkas), H42, pp. 249-294. Berlin: Springer-Verlag.

Hiramoto, Y. (1963). Mechanical properties of sea urchin eggs. I. Surface force and elastic modulus of the cell membrane. *Exp. Cell Res.* **32**, 59-75.

Hoh, J. H. and Schoenenberger, C.-A. (1994). Surface morphology and mechanical properties of MDCK monolayers by atomic force microscopy. *J. Cell Sci.* **107**, 1105-1114.

Hubbe, M. A. (1981). Adhesion and detachment of biological cells in vitro. *Prog. Surf. Sci.* **11**, 65-138.

Ingber, D. E. (1993). The riddle of morphogenesis: a question of solution chemistry or molecular cell engineering? *Cell* **75**, 1249-1252.

Ives, C. L., Eskin, S. G. and McIntire, L. V. (1986). Mechanical effects on endothelial cell morphology: in vitro assessment. *In vitro Cell. Dev. Biol.* **22**, 500-507.

Janmey, P. A. (1991). Mechanical properties of cytoskeletal polymers. *Curr. Opin. Cell Biol.* **2**, 4-11.

Kolega, J. (1986). Effects of mechanical tension on protrusive activity and microfilament and intermediate filament organization in an epidermal epithelium moving in culture. *J. Cell Biol.* **102**, 1400-1411.

Kolega, J., Janson, L. W. and Taylor, D. L. (1991). The role of solation-contraction coupling in regulating stress fiber dynamics in nonmuscle cells. *J. Cell Biol.* **114**, 993-1003.

Kolodney, M. S. and Elson, E. L. (1995). Contraction due to microtubule disruption is associated with increased phosphorylation of myosin regulatory light chain. *Proc. Nat. Acad. Sci. USA* **92**, 10252-10256.

Kreis, T. E. and Birchmeier, W. (1980). Stress fiber sarcomeres of fibroblasts are contractile. *Cell* **22**, 555-561.

Kucik, D. F., Kuo, S. C., Elson, E. L. and Sheetz, M. P. (1991). Preferential attachment of membrane glycoproteins to the cytoskeleton at the leading edge of lamella. *J. Cell Biol.* **114**, 1029-1036.

Lauffenburger, D. A. and Horwitz, A. F. (1996). Cell migration: a physically integrated molecular process. *Cell* **84**, 359-369.

Lee, J., Leonard, M., Oliver, T., Ishihara, A. and Jacobson, K. (1994). Traction forces generated by locomoting keratocytes. *J. Cell Biol.* **127**, 1957-1964.

Lotz, M. M., Burdsal, C. A., Erickson, H. P. and McClay, D. R. (1989). Cell adhesion to fibronectin and tenascin: quantitative measurements of initial binding and subsequent strengthening response. *J. Cell Biol.* **109**, 1795-1805.

Mitchison, T. J. and Cramer, L. P. (1996). Actin-based motility and cell locomotion. *Cell* **84**, 371-379.

Petersen, N. O., McConnaughey, W. B. and Elson, E. L. (1982). Dependence of locally measured cellular deformability on position on the cell, temperature and cytochalasin B. *Proc. Nat. Acad. Sci. USA* **79**, 5327-5331.

Sato, M., Levesque, M. J. and Nerem, R. M. (1987). An application of the micropipette technique to the measurement of the mechanical properties of cultured bovine aortic endothelial cells. *J. Biomech. Eng.* **109**, 27-34.

Sato, M., Theret, D. P., Wheeler, L. T., Ohshima, N. and Nerem, R. M. (1990). Application of the micropipette technique to the measurement of cultured porcine aortic endothelial cell viscoelastic properties. *J. Biomech. Eng.* **112**, 263-268.

Schiro, J. A., Chan, B. M. C., Roswit, W. T., Kassner, P. D., Pentland, A. P., Hemler, M. E., Elsen, A. Z. and Kupper, T. S. (1991). Integrin $\alpha_2\beta_1$ (VLA-2) mediates reorganization and contraction of collagen matrices by human cells. *Cell* **67**, 403-410.

Shirinsky, V. P., Antonov, A. S., Birukov K. G., Sobolevsky A. V., Romanov, Y. A., Kabaeva, N. V., Antonova, G. N. and Smirnov, V. N. (1989). Mechano-chemical control of human endothelium orientation and size. *J. Cell Biol.* **109**, 331-339.

Thoumine, O., Ziegler, T., Girard, P. R. and Nerem, R. M. (1995). Elongation of confluent endothelial cells in culture: the importance of fields of force in the associated alterations of their cytoskeletal structure. *Exp. Cell Res.* **219**, 427-441.

Thoumine, O. and Ott, A. (1996). Influence of adhesion and cytoskeletal integrity on fibroblast traction. *Cell Motil. Cytoskel.* **35**, 269-280.

Thoumine, O., Ott, A. and Louvard, D. (1996). Critical centrifugal forces induce adhesion rupture or structural reorganization in cultured cells. *Cell Motil. Cytoskel.* **33**, 276-287.

Tran-Son-Tay, R., Needham, D., Teung, A. and Hochmuth, R. M. (1991). Time-dependent recovery of passive neutrophils after large deformation. *Biophys. J.* **60**, 856-866.

Truskey, G. A. and Pirone, J. S. (1990). Effect of fluid shear stress upon cell adhesion to fibronectin-treated surfaces. *J. Biomed. Mat. Res.* **24**, 1333-1353.

Valberg, P. A. and Albertini, D. F. (1985). Cytoplasmic motions, rheology, and structure probed by a novel magnetic particle method. *J. Cell Biol.* **101**, 130-140.

Valberg, P. A. and Feldman, H. A. (1987). Magnetic particle motions within living cells. Measurement of cytoplasmic viscosity and motile activity. *Biophys. J.* **52**, 551-561.

Wang, N., Butler, J. P. and Ingber, D. E. (1993). Mechanotransduction across the cell surface and through the cytoskeleton. *Science* **260**, 1124-1127.

Wang, N. and Ingber, D. E. (1994). Control of cytoskeletal mechanics by extracellular matrix, cell shape, and mechanical tension. *Biophys. J.* **66**, 2181-2189.

Watson, P. A. (1991). Function follows form: generation of intracellular signals by cell deformation. *FASEB J.* **5**, 2013-2019.

Wysolmerski, R. B. and Lagunoff, D. (1990). Involvement of myosin light-chain kinase in endothelial cell retraction. *Proc. Nat. Acad. Sci. USA* **87**, 16-20.

Yanai, M., Kenyon, C. M., Butler, J. P., Macklem, P. T. and Kelly, S. M. (1996). Intracellular pressure is a motive force for cell motion in amoeba proteus. *Cell Motil. Cytoskel.* **33**, 22-29.

Zhelev, D. V. and Hochmuth, R. M. (1994). Human neutrophils under mechanical stress. In *Cell Mechanics and Cellular Engineering* (ed. V. C. Mow, F. Guilak, R. Tran-Son-Tay and R. M. Hochmuth). pp. 3-20. Berlin: Springer-Verlag.

Zheng, J., Buxbaum, R. E. and Heidemann, S. R. (1993). Investigation of microtubule assembly and organization accompanying tension-induced neurite initiation. *J. Cell Sci.* **104**, 1239-1250.

Ziemann, F., Rädler, J. and Sackmann, E. (1994). Local measurements of viscoelastic moduli of entangled actin networks using an oscillating magnetic bead micro-rheometer. *Biophys. J.* **66**, 2210-2216.

(Received 5 May 1997 - Accepted 16 June 1997)